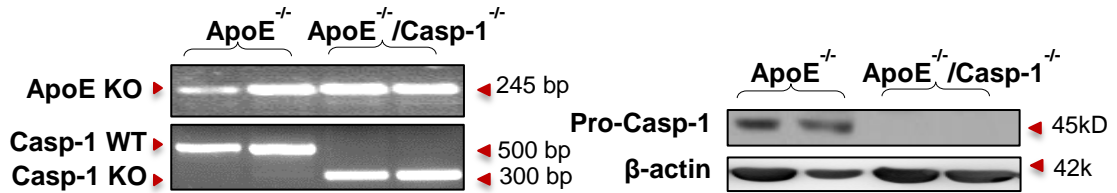
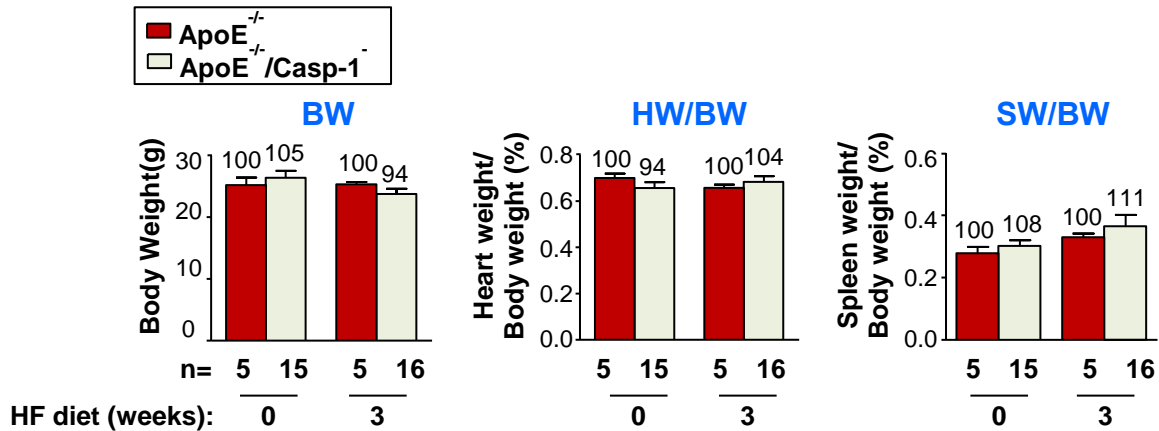


A.



B.



C.

	Cholesterol (mg/dl)		Triglyceride (mg/dl)	
	Normal Chow	HF3w	Normal Chow	HF3w
ApoE^{-/-}	220 ± 67.5 (n=6)	587 ± 120.5 (n=3)	257.2 ± 55.5	289 ± 13.7
ApoE^{-/-}/Casp-1^{-/-}	320.4 ± 64.6 (n=5)	623.25 ± 85.5 (n=4)	303 ± 28.2	328 ± 99.3

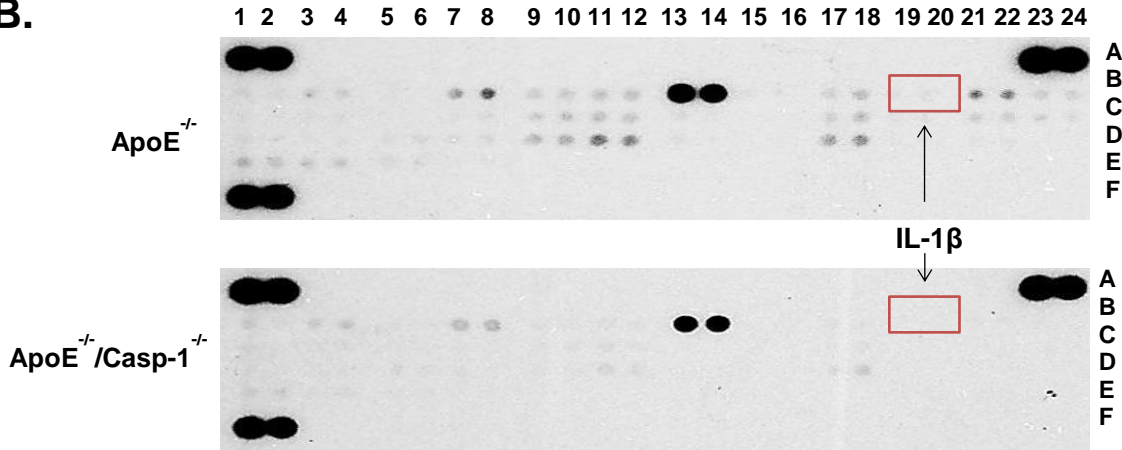
(P>0.05, no statistical differences between the groups)

Figure I. Genotyping and characterization of ApoE^{-/-}Casp-1^{-/-} mice. **A.** Polymerase chain reaction (PCR) analysis of ApoE and caspase-1 (casp-1) gene expressions in ApoE^{-/-} mice and ApoE^{-/-}/Casp-1^{-/-} mice (left panel). Western blot analysis of pro-casp-1 expression in the aortas of ApoE^{-/-} mice and ApoE^{-/-}/Casp-1^{-/-} mice (right panel) (n=2). **B.** General phenotype of Casp-1 deficiency in ApoE^{-/-} mice after 0 or 3 weeks of HF diet: body weight (BW), ratio of heart weight (HW) to BW, and ratio of spleen weight (SW) to BW. **C.** Plasma levels of cholesterol and triglycerides in ApoE^{-/-} mice and ApoE^{-/-}/Casp-1^{-/-} mice after 3 weeks of HF diet (HF3w).

A.

	1	2	3	4	5	6	7	8	9	10	11	12	13	14	15	16	17	18	19	20	21	22	23	24
A	PC																						PC	
B	CXCL13	C5a	G-CSF		GM-CSF		CCL1	CCL11		sICAM-1		IFN- γ		IL-1 α	IL-1 β	IL-1ra		IL-2						
C	IL-3	IL-4	IL-5	IL-6		IL-7	IL-10	IL-13		IL-12p70		IL-16	IL-17	IL-23		IL-27								
D	CXCL10	CXCL11	CXCL1	M-CSF		CCL2	CCL12		CXCL9		CCL3		CCL4	MIP-2		CCL5		CXCL12						
E	CCL17	TIMP-1	TNF- α		TREM-1																			
F	PC																						NC	

B.



C.

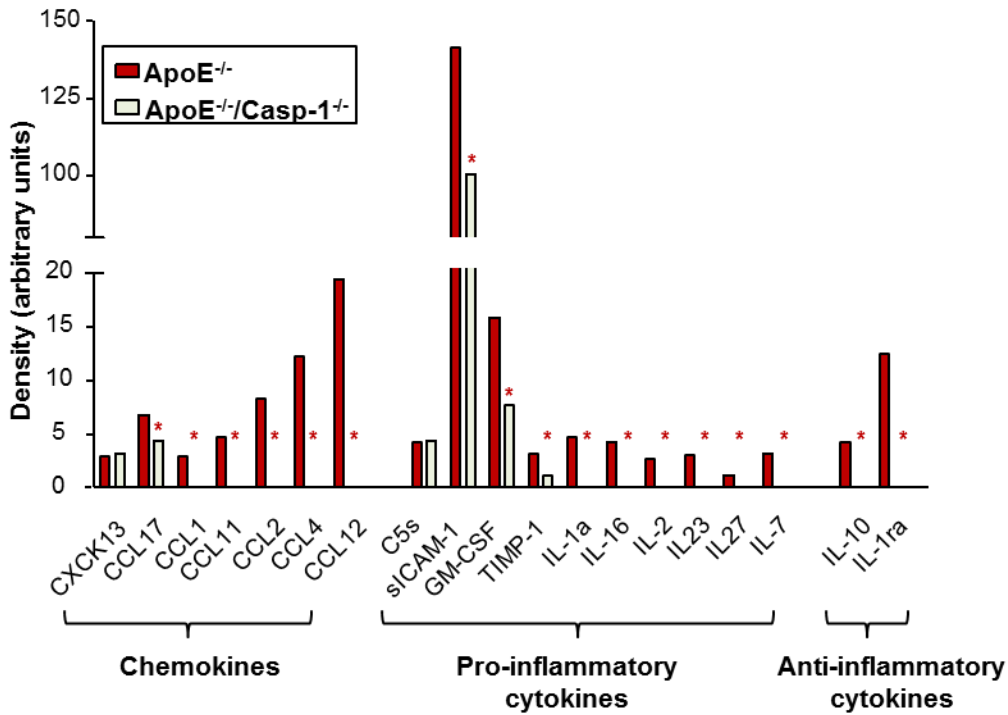


Figure II. Caspase-1 Deficiency Attenuates Cytokine and Chemokine Expression in ApoE^{-/-/Casp-1^{-/-} Mouse Aorta.} **A.** Layout of the cytokine and chemokine array (R&D system). **B.** The representative array images of the aortic lysates from ApoE^{-/-} mice or ApoE^{-/-/Casp-1^{-/-} mice. Two aortas were pooled together for blotting each array. The signal areas of a caspase-1 substrate, IL-1 β , in two arrays were selectively highlighted with red boxes. **C.** The quantification of cytokine and chemokine expressions. The variations of the manufacturer's designate positive control (PC) spots between each array were used to determine the confidence interval of non-specific variations between samples (n=4 for each group). *, p<0.05 indicates the expression changes with statistical significance.}

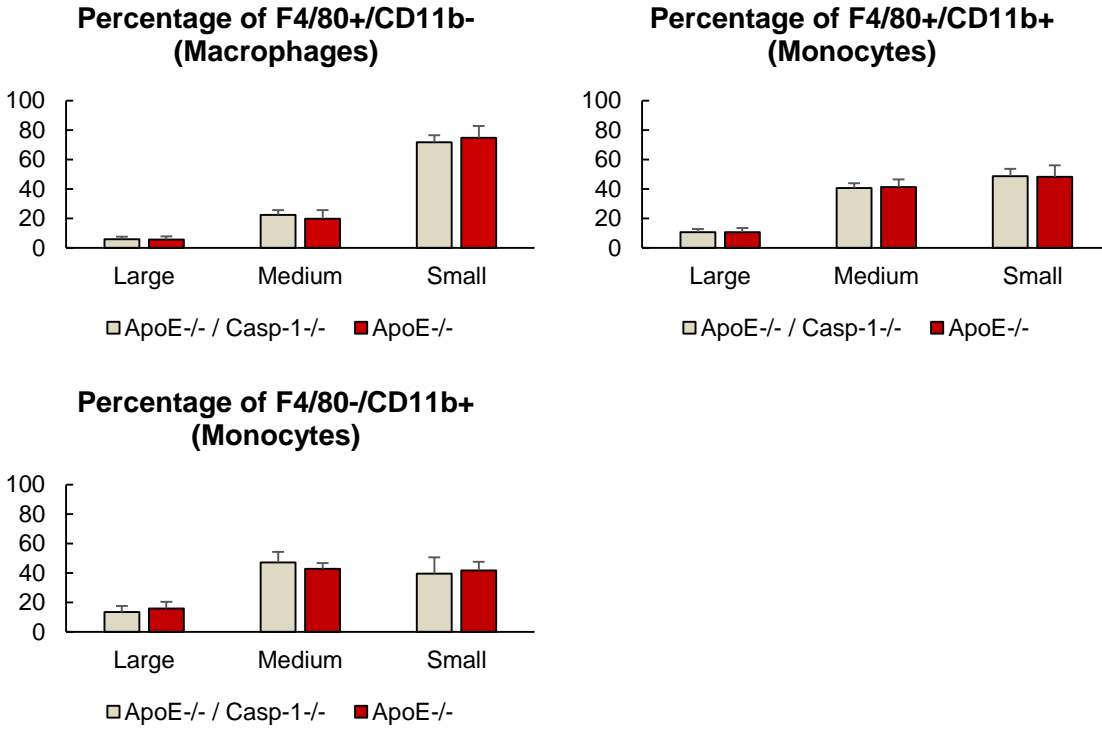
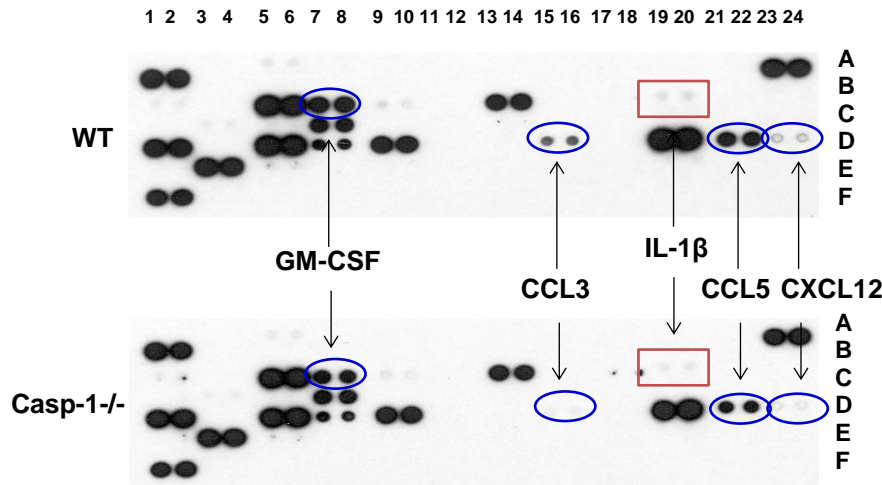


Figure III. No differences are found between the proliferation of macrophages/monocytes in ApoE^{-/-} Casp-1^{-/-} mouse aortas and that of ApoE^{-/-} mice as reflected by the cell size. Cell size is determined with the scales of forward scatter by flow cytometry as an estimate of cell proliferation status.

A.

	1	2	3	4	5	6	7	8	9	10	11	12	13	14	15	16	17	18	19	20	21	22	23	24
A	PC																							PC
B	CXCL13	C5a	G-CSF	GM-CSF	CCL1	CCL11	sICAM-1	IFN- γ	IL-1 α	IL-1 β	IL-1ra	IL-2												
C	IL-3	IL-4	IL-5	IL-6	IL-7	IL-10	IL-13	IL-12p70	IL-16	IL-17	IL-23	IL-27												
D	CXCL10	CXCL11	CXCL1	M-CSF	CCL2	CCL12	CXCL9	CCL3	CCL4	MIP-2	CCL5	CXCL12												
E	CCL17	TIMP-1	TNF- α	TREM-1																				
F	PC																							NC

B.



C.

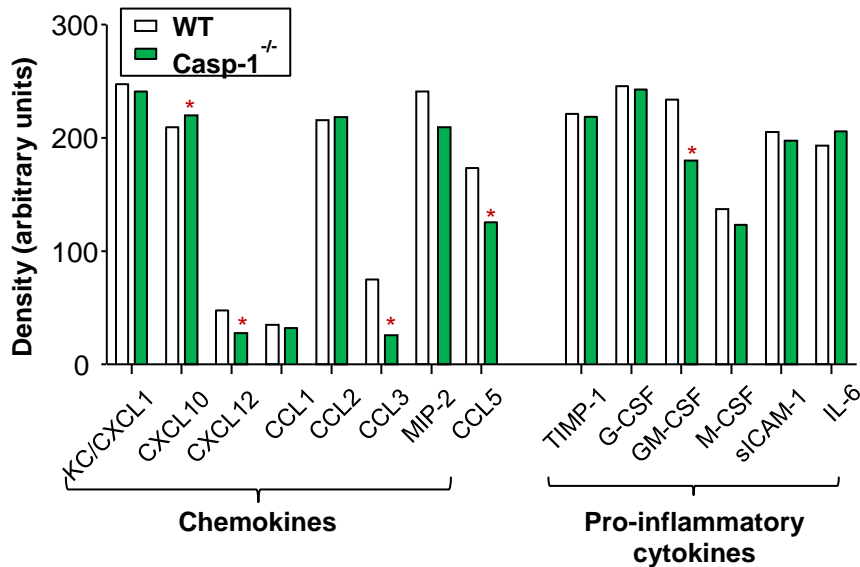


Figure IV. Caspase-1 Promotes Secretome of Pro-inflammatory Cytokines and Chemokines in MAECs. **A.** Layout of the cytokines and chemokine array purchased from R&D systems. **B.** Array images of the culture supernatant from WT MAECs or Casp-1^{-/-} MAECs cultured and primed with 50ng/ml LPS and treated with 200 μ g/ml oxLDL for 24 hours followed with ATP (5mM) spike for 20 min. The array spots of IL-1 β were highlighted with the red boxes where the array spots of GM-CSF, CCL3, CCL5 and CXCL12 were indicated with the black ovals, respectively. **C.** The quantification of cytokine and chemokine expressions. The variations of the manufacturer's designate positive control (PC) spots between each array were used to determine the confidence interval of non-specific variations between samples (n=2 for each group). *, $p < 0.05$ change with significance.

A. NIH-NCBI BLAST homology

1	MADEVALALQAAGSPSAAAA-MEASQPADEPLRKRPRRDGPGGLGRSPGEPSSAA-----V	54
1	MADE ALALQ GSPSAA A EAAS PA EPLRKRPRRDGPGGL RSPGEP A V	
1	MADEAALALQPGGSPSAAAGADREAAASSPAGEPLRKRPRRDGPGGLERSPGEPGGAAPEREV	60
55	APAAAGCEAASAAAPALWREAAGAAASAEREAPATAVAGDGDNGSGLR---REPRRAADD	111
61	AA GC A+AAA A AA + ATA AG+GDNG GL+ REP AD+	
61	PAARAGCPGAAAAALWREAEEAAAAGGEQEAQ-ATAAAGEGDNGPGGLQGPSREPPPLADN	119
Mouse SIRT1	112 FDDDEGEDEEAAAAAAAAAIGYRDNLLLTGLLTNGFHSCESDDDDRTSHASSSDWTFR	171
Human SIRT1	120 LYDEDDDEGEDEEAAAAAAAAAIGYRDNLLFGEIITNGFHSCESDEEDRASHASSSDWTFR	179
172	PRIGPYTFVQQHLMIGTDPRTILKDLLPETIPPELDDMTLWQIVINILSEPPKRRKRRKD	231
180	PRIGPYTFVQQHLMIGTDPRTILKDLLPETIPPELDDMTLWQIVINILSEPPKRRKRRKD	239
232	INTIEDAVKLLQECKKIIIVLTGAGVSVSCGIPDFRSRDGIYARLAVDFPDLDPQAMFDI	291
240	INTIEDAVKLLQECKKIIIVLTGAGVSVSCGIPDFRSRDGIYARLAVDFPDLDPQAMFDI	299
292	EYFRKDPFPFFKFAKEIYPGQFQPSLCHKFIALSDKEGKLLRNYTQNMIDTLEQVAGIQRI	351
300	EYFRKDPFPFFKFAKEIYPGQFQPSLCHKFIALSDKEGKLLRNYTQNMIDTLEQVAGIQRI	359
352	LQCHGSFATASCLICKYKVDCEAVRGDIFNQVVRCPRCPPADEPLAIMKPEIVFFGENLP	411
360	IQCHGSFATASCLICKYKVDCEAVRGDIFNQVVRCPRCPPADEPLAIMKPEIVFFGENLP	419
412	EQFHRAMKYDKDEVDLLIVIGSSLKVRPVALIPSSIPHEVPQILINREPLPHLHFDVELL	471
420	EQFHRAMKYDKDEVDLLIVIGSSLKVRPVALIPSSIPHEVPQILINREPLPHLHFDVELL	479
472	GDCDVIINELCHRLGGEYAKLCCNPVKLSEITEKPPRPQKELVHLSLPPPTPLHISEDSS	531
480	GDCDVIINELCHRLGGEYAKLCCNPVKLSEITEKPPRTQKELAYLSLPPPTPLHVSSEDSS	539
532	SPERTVPQDSSVIATLVDQATNNVNDLEVSES-SCVEEKPOEVQTSRNVENI--NVENP	588
540	SPERT P DSSVI TL+DQA +N +DL+VSES C+EEKPOEVQTSRNV+I +ENP	
540	SPERTSPDSSVIVTLLDQAASN-DLDVSESKGCMEKPOEVQTSRNVESIAEQMENP	598
589	DFKAVGSSSTADKNERTSVAETVRKWCWPNRLAKEQISKRLEGNQYLFVPPNRYIFHGAEVY	648
599	DLKNVGSSTGKKNERTSVAGTVRKCWPNRVAKEQISRRLDGNQYLFVPPNRYIFHGAEVY	658
649	SDSEDDVLSSSSSCGSNSDSGTCQSPSLEEPLEDESEIEEFYNGLEDTERPECAGGSGFG	708
659	SDSEDDVLSSSSSCGSNSDSGTCQSPSLEEPMEDESEIEEFYNGLED+ + PE AGG+GFG	718
709	ADGGDQEVVNEAIAIRQELTDVNYPSDKS 737	
	DG DQE +NEAI+ +QE+TD+NYPSS+KS	
719	TDGDDEAINEAISVKQEVTDVNYPSNKS 747	

Species	Casp1 Cleavage Site
Mouse SIRT1	D142 (Chalkiadaki, A, et al. Cell Metab., 2012)
Human SIRT1	D150 (BLAST search and confirmation by our previously published method: Shen, J, et al. Atherosclerosis, 2008)

B.

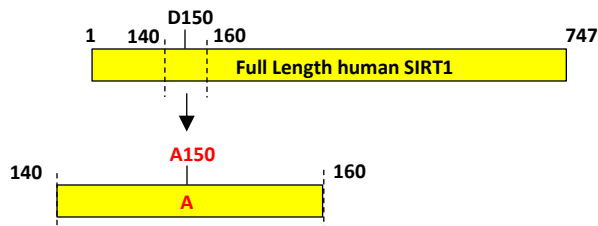


Figure V. Generation of Cell-permeable non-Casp1 cleavable Sirt1 polypeptide. A. NIH-NCBI Blast homology search between mouse SIRT1 (upper) and human SIRT1 (lower). Caspase-1 cleavage site is highlighted in the red box. B. The non-cleavable Sirt1 polypeptide was generated with a single amino acid replacement in the sequence from 140-160 position of human SIRT1. Caspase-1 cleavage site D150 from human SIRT1 was mutated to A150, rendering the peptide sequence non-casp1 cleavable.

Name of enzyme	Predicted No. of cleavages	Predicted Positions of cleavage sites	Regulated by Apocynin	PMID
Caspase-1	1	528	Yes	N/A
Caspase-3	1	242	Yes	19592621
Caspase-7	1	242	Not Tested	N/A
Thrombin	1	202	Not Tested	N/A
Caspase-10	0			N/A
Caspase-2	0			N/A
Caspase-4	0			N/A
Caspase-5	0			N/A
Caspase-6	0			N/A
Caspase-8	0			N/A
Caspase-9	0			N/A
Enterokinase	0			N/A
Factor Xa	0			N/A
Granzyme B	0			N/A

Table I. Predicated proteinases for human Sirt1 protein cleavage. The analysis with the PeptideCutter database predicted potential proteinases for human Sirt1 protein cleavages. Data are expressed as mean \pm SE. *, $p < 0.05$, changes with statistical significance.

A.

Gene ID	PMID (Ap1 Target genes)	Fold Change	Microarray data obtained via mining		
			p	Comparison	PMID
CCL1*†	22311973	1.456	0.0084	Sirt1 (-/-) vs. WT	22715468
CCL2*	8630731	2.364	0.0155	Sirt1 (-/-) vs. WT With HFD	
CCL3†	14747532	8.623	0.0000	Sirt1 (-/-) vs. WT With HFD	22883230
CCL4*	18789903	2.736	0.0000	Sirt1 (-/-) vs. WT With HFD	
CCL17*	14747532	1.591	0.0010	Sirt1 (-/-) vs. WT With LFD	
GM-CSF*†	9190901	2.265	0.0084	Sirt1(-/+) vs. Sirt1(+/+)	22006157
CXCL12†	17393416	1.813	0.0172	Sirt1 (-/-) vs. WT	22169038
IL2*	1737937	1.184	0.0469	Sirt1 (-/-) vs. WT With LFD	22883230
		1.339	0.0258	Sirt1 (-/-) vs. WT	22715468
		1.372	0.0024	Sirt1 (-/-) vs. WT	
EBI3 (IL27)*	15728491	1.484	0.0032	Sirt1 (-/-) vs. WT With HFD	
		2.014	0.0004	Sirt1 (-/-) vs. WT With LFD	
		3.018	0.0021	Sirt1 (-/-) vs. WT With HFD	22883230
TIMP1*	10051488	1.435	0.0068	Sirt1 (-/-) vs. WT With LFD	
		1.638	0.0003	Sirt1 (-/-) vs. WT With HFD	
		1.169	0.0445	Sirt1 (-/-) vs. WT With LFD	
VCAM1‡	1379595	1.824	0.0285	Sirt1 (-/-) vs. WT	22169038
		1.433	0.0213	Sirt1 (-/-) vs. WT	
		1.306	0.0055	Sirt1 (-/-) vs. WT With LFD	
IL16*	9990060	3.764	0.0054	Sirt1 (-/-) vs. WT With LFD	22883230
		1.317	0.0248	Sirt1 (-/-) vs. WT With LFD	
CCL12*	Not found	2.262	0.0115	Sirt1(-/+) vs. Sirt1(+/+)	22006157

B.

Gene	Fold Change	p	Compares	PMID
Jun	1.778	0.000495	Sirt1 KO vs. WT with LFD	22883230
Fos	3.523	0.017899	Sirt1 KO vs. WT with LFD	22883230
Fos1	3.022	0.000628	Sirt1 KO vs. WT with HFD	22883230

Table II. Caspase-1 induces upregulation of proinflammatory cytokines, chemokines and adhesion molecules via sirtuin 1 (Sirt1)-AP-1 pathway. **A.** Caspase-1-induced molecules have the AP-1 binding site in their promoters and Sirt1 gene deficiency increases the expression of caspase-1-induced molecules. The list of PubMed IDs showed that published papers experimentally identified AP-1 binding site in their promoters of caspase-1 induced genes except CCL-12 and IL-7. The database mining analysis of published microarray data of Sirt1 gene deficient (-/-) mice versus wild-type control mice demonstrated that Sirt1 deficiency increases the expression of caspase-1-induced genes. The symbols indicate the figures, in which the results showed that caspase-1 induced the gene upregulation/secretion: *Figure S2, †Figure S4, ‡Fig.4). **B.** Sirtuin 1 deficiency increases the expression of AP-1 gene expression. The AP-1 subunits expression was retrieved from Sirt1 KO (knockout) microarray dataset GSE30247.